//Blrnas1/journals/application/oup/PCP/pcs059.3d [28.4.2012–4:21am] [1–10] Paper: pcs059
MANUSCRIPT CATEGORY: REGULAR PAPER

PCP
PLANT & CELL PHYSIOLOGY

Functional Characterization of Residues Involved in Redox Modulation if Maize Photosynthetic NADP-Malic Enzyme Activity

Q1

Clarisa E. Alvarez[1], Enrique Detarsio[1], Silvia Moreno[2], Carlos S. Andreo[1] and María F. Drincovich[1,*]

[1]Centro de Estudios Fotosintéticos y Bioquímicos (CEFOBI), Universidad Nacional de Rosario, Suipacha 531, Rosario, Argentina
[2]Departamento de Química Biológica, Facultad de Ciencias Exactas y Naturales, Universidad de Buenos Aires, Ciudad Universitaria, Pabellón 2, 1428 Buenos Aires, Argentina
*Corresponding author: E-mail, drincovich@cefobi-conicet.gov.ar; Fax, +543144370044.
(Received January 7, 2012; Accepted April 11, 2012)

Regular Paper

Two highly similar plastidic NADP-malic enzymes (NADP-MEs) are found in the C_4 species maize (*Zea mays*); one exclusively expressed in the bundle sheath cells (BSCs) and involved in C_4 photosynthesis (ZmC_4-NADP-ME); and the other ($ZmnonC_4$-NADP-ME) with housekeeping roles. In the present work, these two NADP-MEs were analyzed regarding their redox-dependent activity modulation. The results clearly show that ZmC_4-NADP-ME is the only one modulated by redox status, and that its oxidation produces a conformational change limiting the catalytic process, although inducing higher affinity binding of the substrates. The reversal of ZmC_4-NADP-ME oxidation by chemical reductants suggests the presence of thiol groups able to form disulfide bonds. In order to identify the cysteine residues involved in the activity modulation, site-directed mutagenesis and MALDI-TOF (matrix-assisted laser desorption ionization-time of flight) analysis of ZmC_4-NADP-ME were performed. The results obtained allowed the identification of Cys192, Cys246 (not conserved in $ZmnonC_4$-NADP-ME), Cys270 and Cys410 as directly or indirectly implicated in ZmC_4-NADP-ME redox modulation. These residues may be involved in forming disulfide bridge(s) or in the modulation of the oxidation of critical residues. Overall, the results indicate that, besides having acquired a high level of expression and localization in BSCs, ZmC_4-NADP-ME displays a particular redox modulation, which may be required to accomplish the C_4 photosynthetic metabolism. Therefore, the present work could provide new insights into the regulatory mechanisms potentially involved in the recruitment of genes for the C_4 pathway during evolution.

Keywords: C_4 photosynthesis • Maize • NADP-malic enzyme • Redox modulation • Structure–function relationship.

Abbreviations: BSC, bundle sheath cell; CD, circular dichroism; DTT, dithiothreitol; IBZ, iodosobenzoate; MALDI-TOF, matrix-assisted laser desorption ionization-time of flight; MS, mass spectrometry; NADP-ME, NADP-malic enzyme; ZmC_4-NADP-ME, maize photosynthetic NADP-ME; $ZmnonC_4$-NADP-ME, maize non-photosynthetic plastidic NADP-ME.

Introduction

The decarboxylation of C_4 acids in the bundle sheath cells (BSCs) is a key step in the photosynthetic process of C_4 plants. Depending on the C_4 species, this process can be mediated by NADP-malic enzyme (NADP-ME), NAD-malic enzyme and/or phosphoenolpyruvate carboxykinase (Kanai and Edwards 1999, Drincovich et al. 2011). During the last few years, remarkable advances have been made in the characterization of different isoforms of each C_4 decarboxylase. In most cases, non-photosynthetic isoforms of the C_4 decarboxylating enzymes involved in primary and/or secondary metabolism were characterized. These isoforms were the starting point for the evolution of the photosynthetic C_4-specific decarboxylases. During this evolutionary process, C_4 enzymes have acquired characteristics that make them more suitable to fulfill the requirements of the C_4 photosynthetic process (Ku et al. 1996, Drincovich et al. 2001, Drincovich et al. 2011).

In many C_4 species, such as maize, sugarcane and sorghum, NADP-ME (EC 1.1.1.40) is the unique or major decarboxylase and malate is the predominant C_4 acid formed during photosynthesis. This enzyme catalyzes the oxidative decarboxylation of L-malate to yield carbon dioxide and pyruvate with the concomitant reduction of NADP (Edwards and Andreo 1992, Drincovich et al. 2001). In maize, the photosynthetic NADP-ME (ZmC_4-NADP-ME) is exclusively expressed in the BSC chloroplasts (Maurino et al. 1997, Maurino et al. 2001, Saigo et al. 2004, Detarsio et al. 2008), and displays particular kinetic, structural and regulatory properties (Detarsio et al. 2003, Detarsio et al. 2007). Apart from ZmC_4-NADP-ME, other NADP-ME isoforms not involved in the photosynthetic process are expressed in maize (Drincovich et al. 2001, Saigo et al. 2004, Detarsio et al. 2008). One of these isoforms, maize

Plant Cell Physiol. 0(0): 1–10 doi:10.1093/pcp/pcs059, available online at www.pcp.oxfordjournals.org

//Blrnas1/journals/application/oup/PCP/pcs059.3d [28.4.2012–4:21am] [1–10] Paper: pcs059
MANUSCRIPT CATEGORY: REGULAR PAPER

non-photosynthetic NADP-ME (ZmnonC$_4$-NADP-ME), is constitutively expressed in maize plastids and plays housekeeping roles; representing the more recent and direct ancestor of ZmC$_4$-NADP-ME (Tausta et al. 2002, Saigo et al. 2004). Although the two maize plastidic NADP-MEs share 85% identity, they show distinctive differences (Detarsio et al. 2007). The most relevant structural difference is the oligomeric state; ZmC$_4$-NADP-ME assembles as a tetramer and ZmnonC$_4$-NADP-ME as a dimer. Regarding kinetic properties, one of the most outstanding peculiarities is ZmC$_4$-NADP-ME inhibition by the substrate malate in a pH-dependent way (Drincovich and Andreo 1992); while ZmnonC$_4$-NADP-ME is not inhibited at all (Detarsio et al. 2007). Thus, high malate levels found in C$_4$ plant tissues, along with the pH decrease in the chloroplast stroma when photosynthesis is off, would both produce a reduction in the C$_4$ NADP-ME activity.

Redox regulation plays a key role in many plastid functions. Chloroplasts undergo changes in redox potential during the day/night cycle as well as during variations in metabolic demands. In this regard, NADP-ME purified from maize leaves is inactivated by cysteine oxidants (Drincovich et al. 1992, Drincovich and Andreo 1994). Moreover, NADP-ME activity increases in maize leaves due to illumination, which has been suggested to be due to a change in the redox state of cysteine residues (Murmu et al. 2003). However, the analysis of the redox modulation of the various NADP-ME isoforms, which are co-expressed in maize leaves (Saigo et al. 2004, Detarsio et al. 2007), has not been performed yet. Thus, in the present work, redox activity modulation of the two plastidic ZmNADP-ME isoforms from leaves was analyzed using recombinant purified proteins. The results obtained indicate a specific redox regulation of ZmC$_4$-NADP-ME activity, modulation that is not observed in the case of ZmnonC$_4$-NADP-ME. Moreover, the specific amino acids responsible for ZmC$_4$-NADP-ME redox regulation were mapped, and the location of cysteine residues in NADP-MEs from other species were in silico analyzed. Overall, the results indicate that, besides acquiring a high level of expression and localization in BSCs, ZmC$_4$-NADP-ME displays a particular redox modulation of its activity, which may be required to accomplish the C$_4$ photosynthetic metabolism successfully.

Results

Redox modulation of recombinant ZmC$_4$- and ZmnonC$_4$-NADP-ME activity

Purified recombinant ZmC$_4$- and ZmnonC$_4$-NADP-ME were incubated with chemical oxidants in order to assess the redox modulation of their activities (**Fig. 1A**). Three different oxidants that differ in redox potentials were used: iodosobenzoate (IBZ) and $CuCl_2$, which are highly oxidative agents; and diamide, which has been widely used to induce the formation of disulfides (Kosower and Kosower 1987). The results show a time-dependent decrease of ZmC$_4$-NADP-ME activity in the presence of the three oxidants, reaching nearly 40% of activity at 60 min of incubation in all cases (**Fig. 1A**). In contrast, ZmnonC$_4$-NADP-ME activity is not significantly modified by any chemical oxidant, at least until 60 min of incubation (**Fig. 1A**).

In order to asses the reversal of ZmC$_4$-NADP-ME inactivation, the enzyme was incubated with diamide for 20 min (60% of initial activity), desalted and further incubated with the reductant dithiothreitol (DTT; **Fig. 1B**). In the presence of

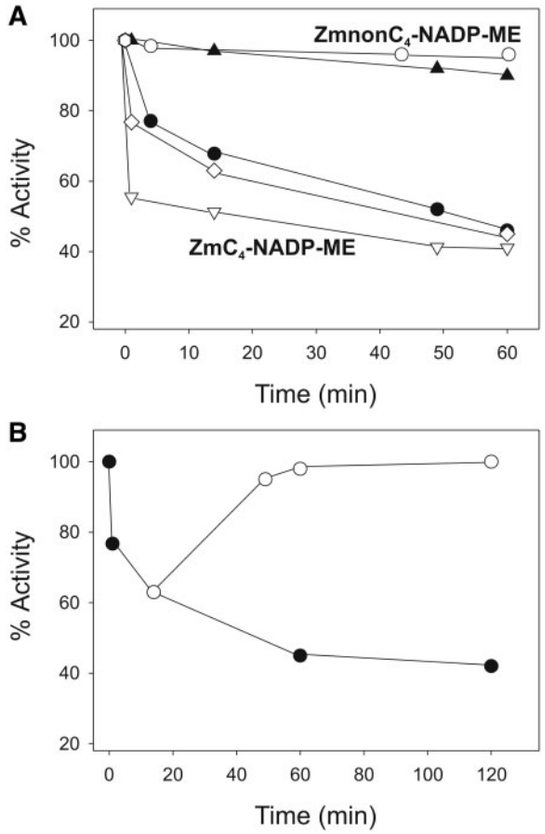

Fig. 1 Redox modulation of recombinant maize NADP-MEs. (A) Recombinant ZmC$_4$-NADP-ME was incubated with either 1 mM IBZ (open inverted traingles), 2 mM diamide (filled circles) or 25 μM $CuCl_2$ (open diamonds). ZmnonC$_4$-NADP-ME was incubated with either 1 mM IBZ (open circles) or 25 μM $CuCl_2$ (filled upright triangles). At several time points, NADP-ME activity was measured and expressed as a perncetage of the initial activity. (B) ZmC$_4$-NADP-ME was incubated with 2 mM diamide (filled circles) and enzyme activity was measured at different times. When approximately 60% of initial activity was reached, an aliquot was desalted and further incubated with 10 mM DTT (open circles). For each time course incubation experiment, typical results are shown from at least three different incubation experiments using different preparations, in which similar results were obtained. In each incubation experiment, the activity was measured once at the indicated time intervals. In each experiment the initial activity of ZmC$_4$-NADP-ME was 200 ± 15 U mg^{-1} and that of ZmnonC$_4$-NADP-ME was 180 ± 10 U mg^{-1}.

//Blrnas1/journals/application/oup/PCP/pcs059.3d [28.4.2012–4:21am] [1–10] Paper: pcs059
MANUSCRIPT CATEGORY: REGULAR PAPER

PCP PLANT & CELL PHYSIOLOGY

DTT, a complete recovery of the initial NADP-ME activity is observed after 90 min of incubation (**Fig. 1B**).

Kinetic and structural properties of oxidized and reduced ZmC_4-NADP-ME

Kinetic parameters of reduced and oxidized ZmC_4-NADP-ME were estimated at two pH values, i.e. 7.0 and 8.0. ZmC_4-NADP-ME was incubated with 10 mM DTT for 2 h (redZmC_4-NADP-ME) or with 2 mM diamide for 20 min (oxZmC_4-NADP-ME) and desalted. The results indicate that ZmC_4-NADP-ME oxidation decreases the catalytic activity at both pH values tested (**Table 1**). On the other hand, a decrease in K_m values for NADP of nearly three or four times is detected after oxidation, while K_m values for malate measured at both pH values decreased nearly 2-fold after oxidation (**Table 1**). In the case of ZmnonC_4-NADP-ME, kinetic parameters were not significantly modified after incubation with DTT or diamide (not shown).

The oligomeric state of red- and oxZmC_4-NADP-MEs was also analyzed by native gel electrophoresis (Detarsio et al. 2007). The enzyme treated with either DTT or diamide shows the same mobility in native electrophoresis, with a molecular mass consistent with a tetramer in all cases (**Supplementary Fig. S1**). In addition, circular dichroism (CD) spectra were determined for red- and oxZmC_4-NADP-MEs. The CD spectra obtained were superimposable, indicating that no severe loss of protein secondary structure takes place after ZmC_4-NADP-ME oxidation (**Supplementary Fig. S2A**).

Functional characterization of ZmC_4-NADP-ME cysteine residues

ZmC_4-NADP-ME and ZmnonC_4-NADP-ME share nearly 85% protein identity (**Fig. 2**). From the seven cysteine residues found in ZmC_4-NADP-ME (Cys192, Cys231, Cys246, Cys270, Cys410, Cys499 and Cys625), only one (Cys246) is not conserved in ZmnonC_4-NADP-ME (**Fig. 2**). A prediction of the three-dimensional model of ZmC_4-NADP-ME based on the crystallographic data for the human mitochondrial NAD(P)-ME complexed with its substrates (1EFL from the Protein Data Bank; http://www.rcsb.org/pdb/; Detarsio et al. 2004) was analyzed regarding the position of the seven cysteine residues (**Fig. 3A**). The relative position among the seven residues as well as the spatial relationship with respect to the substrate-binding site were taken into account to select residues that could be involved in the redox modulation of the enzyme. The predicted model shows that Cys192, Cys231, Cys246 and Cys270 are close enough to participate in a disulfide bridge (**Fig. 3A**). On the other hand, and based on this model, Cys410, Cys499 and Cys625 are far away from the enzyme active site and from other cysteine residues (**Fig. 3A**). Thus, four cysteine residues, i.e. Cys192, Cys231, Cys246 and Cys270, were selected for site-directed mutagenesis analysis, replacing them with alanine residues.

Purification and structural characterization of ZmC_4-NADP-ME mutants

Four different ZmC_4-NADP-ME mutants were constructed by replacing cysteine residues with alanine: C192A, C231A, C246A and C270A. Although expressed to lower levels than the wild type, the mutated NADP-MEs were successfully expressed in *Escherichia coli* BL21(DE3) and purified to homogeneity using the same procedure previously described for the mature wild-type NADP-ME (not shown; Detarsio et al. 2003). The oligomeric state of ZmC_4-NADP-ME mutants was analyzed by native gel electrophoresis (Detarsio et al. 2007). The four mutants show the same mobility in native electrophoresis as the wild type, with a molecular mass consistent with a tetramer (not shown). The mobility in native gel electrophoresis of C231A in comparison with the wild type is shown in **Supplementary Fig. S1**.

To determine whether the introduced mutations resulted in a loss of overall structural integrity, CD spectra were obtained for all mutant proteins and compared with the one obtained for the wild-type NADP-ME. In all cases, the CD spectra were superimposable after corrections were made for protein concentration (**Supplementary Fig. S2B**). In this way, structural changes, if any, should be limited to the active site without generating a severe loss of protein structure.

Kinetic characterization of C192A, C231A, C246 and C270A

The apparent kinetic parameters of the purified recombinant ZmC_4-NADP-ME mutants C192A, C231A, C246A and C270A were estimated and compared with those of the wild type (**Table 2**). All mutants display a marked decrease in k_{cat}, presenting values from 8.6% to 0.4% compared with the wild

Table 1 Kinetic parameters of recombinant oxidized and reduced ZmC_4-NADP-ME at pH 7.0 or 8.0

		k_{cat} (s^{-1})	K_m NADP (μM)	K_m malate (mM)
pH 8.0	redZmC4-NADP-ME	269.0 ± 0.5	27.6 ± 1.2	0.39 ± 0.03
	oxZmC_4-NADP-ME	91.0 ± 8.3	8.8 ± 0.3	0.17 ± 0.01
pH 7.0	redZmC4-NADP-ME	8.35 ± 0.89	14.7 ± 0.6	0.15 ± 0.03
	oxZmC_4-NADP-ME	3.55 ± 0.30	3.6 ± 0.2	0.080 ± 0.008

Purified recombinant ZmC_4-NADP-ME was treated with either 10 mM DTT (redZmC_4-NADP-ME) for 2 h or 2 mM diamide (oxZmC_4-NADP-ME) for 20 min. After the treatment, the enzyme was desalted and kinetic parameters were estimated at pH 8.0 or 7.0. Values are given as average ± SD. Each value is the average obtained using at least three different preparations of each enzyme.

```
ZmC4-NADP-ME       MLSTRTAAVAASASPASPWKLGGRSEGGASCDGCRTYRNTLRRRAAPAKVRALPPRRVDA 60
ZmnonC4-NADP-ME    MISART----AAASPASLWKQGGRSEGGGSCDGCRTYRNTLRR-AAAAKVRALPSRAVEA 55
                   *:*:**    *:***** ** *******.************** **.*******.* *:*

ZmC4-NADP-ME       VAMVSNAETETEKEQEEAAAA-------------SEELPVMPWATSVASGYTLLRDPHHN 107
ZmnonC4-NADP-ME    VKMGSAAEMEQEEAEVAAAAAGVVVEDHYGEDSATEELPILPWAFSVASGYTLLRDPHHN 115
                   * * * ** * *: :  **** :****::*** ***************

ZmC4-NADP-ME       KGLAFTEEERDGHYLRGLLPPAVLSQELQIKKFMNTLRQYQTPLQRYIAMMNLQETDERL 167
ZmnonC4-NADP-ME    KGLAFMEKERDAHHLRGLLPPAVVPQELQIKKIMHNLRQYQVPLQRYMAMMDLQERNERL 175
                   ***** *:***.*:**********:.*******:*:.*****.*****:***:*** :***

ZmC4-NADP-ME       FYKLLIDNVVELLPFVYTPTVGEACQKYGSIFGRPQGLYVSLKDKGKVLEVLRNWPHRNI 227
ZmnonC4-NADP-ME    FYKLLIDNVEELLPVVYTPTVGEACQKYGSIFRQPQGLYVSLRDKGKVLEVLRNWPHRNI 235
                   ********* ****.***************** :********:*****************

ZmC4-NADP-ME       QVICVTDGERILGLGDLGCQGMGIPVGKLALYTALGGVDPSVCLPITIDVGTNNEFLLND 287
ZmnonC4-NADP-ME    QVICVTDGERILGLGDLGSQGMGIPVGKLALYTALGGVRPSACLPITIDVGTNNEKLLND 295
                   ******************.****************** **.************* ****

ZmC4-NADP-ME       EFYIGLRQKRATGEEYDELIEEFMSAVKQFYGEKVLIQFEDFANHNAFDLLEKYSKSHLV 347
ZmnonC4-NADP-ME    EFYIGLRQKRATGEEYHELMEEFMAAVKQIYGEKVLIQFEDFANHNAFNLLAKYSKSHLV 355
                   ****************.**:****:****:********************:** ********

ZmC4-NADP-ME       FNDDIQGTASVVLAGLLAALKMVGGTLAEQTYLFLGAGEAGTGIAELIALEISKQTNAPI 407
ZmnonC4-NADP-ME    FNDDIQGTASVVLAGLLAALKVVGGTLAEHTYLFLGAGEAGTGIAELIALEISKQTSAPI 415
                   **********************:*******:****************************.***

ZmC4-NADP-ME       EECRKKVWLVDSKGLIVDSRKGSLQPFKKPWAHEHEPLKTLYDAVQSIKPTVLIGTSGVG 467
ZmnonC4-NADP-ME    EECRKKIWLVDSKGLIVDSRKNSVQSFKKPWAHEHEPLTTLYDAVQSIKPTVLIGTSGVG 475
                   ******:**************.*:*.************.********************

ZmC4-NADP-ME       RTFTKEIIEAMSSFNERPIIFSLSNPTSHSECTAEQAYTWSQGRSIFASGSPFAPVEYEG 527
ZmnonC4-NADP-ME    RTFTKEVVEAMASFNERPIIFSLSNPTSHSECTAEEAYNWTQGRAIFASGSPFDPVEYDG 535
                   ******::***:************************:**.*:***:******** ****:*

ZmC4-NADP-ME       KTFVPGQSNNAYIFPGLGLGLVISGAVRVHEDMLLAASKALADQATQDNFEKGSIFPPFT 587
ZmnonC4-NADP-ME    KVFVPGQSNNAYIFPGFGLGLVISGAIRVHEDMLLAASEALAAQATQENFDKGSIFPPFT 595
                   *.***************:*********:***********:*** ****:**:*********

ZmC4-NADP-ME       SIRKISAHIAAAVAGKAYELGLATRLPPPSDLVKYAENCMYTPVYRNYR 636
ZmnonC4-NADP-ME    NIRKISARIAAAVAAKAYELGLATRLPPPRDLVKYAQSCMYTPVYRNYR 644
                    .******:******.************** ******:.***********
```

Fig. 2 Sequence alignment of ZmC_4-NADP-ME and $ZmnonC_4$-NADP-ME. The plastidic NADP-ME isoforms from maize ZmC_4-NADP-ME (Rothermel and Nelson 1989) and $ZmnonC_4$-NADP-ME (Saigo et al. 2004) were aligned using CLUSTAL W. Predicted transit peptides are indicated in italics and underlined. Cysteine residues of each enzyme are indicated in bold and highlighted with a gray box. Only Cys246 from ZmC_4-NADP-ME is not conserved in $ZmnonC_4$-NADP-ME and replaced by serine.

type (**Table 2**). With regard to the K_m values for NADP, all mutants show higher affinity for this substrate (**Table 2**). Notably, C246A exhibits a nearly 5-fold increase in its affinity towards NADP. Considering malate, C246A also shows a decrease (nearly 3-fold) in the K_m for this substrate (**Table 2**). However, the other mutants display lower malate affinity than the wild type, with increases between four and 11 times in the K_m for malate (**Table 2**). Thus, all the ZmC_4-NADP-ME cysteine mutants constructed and analyzed show significantly lower catalytic efficiencies for both NADP and malate than the wild type (**Table 2**).

Redox modulation of ZmC_4-NADP-ME mutants activity

Purified recombinant ZmC_4-NADP-ME mutants C192A, C231A, C246A and C270A were incubated with 1 mM IBZ (**Fig. 3B**). The results indicate that while the wild-type ZmC_4-NADP-ME and C231A activities decrease in the presence of the oxidant IBZ, the activity of the mutants C192A, C246A and C270A is not significantly changed until 120 min of incubation with the chemical oxidant (**Fig. 3B**).

MALDI-TOF-MS analysis of oxidized and reduced ZmC_4-NADP-ME

In order to identify further the cysteine residues involved in the modulation of ZmC_4-NADP-ME activity, $oxZmC_4$-NADP-ME (treated with 2 mM diamide) and $redZmC_4$-NADP-ME (treated with 10 mM DTT) were analyzed by matrix-assisted laser desorption ionization-time of flight mass spectrometry(MALDI-TOF-MS) (**Fig. 4**). The pattern of peptides obtained for both enzymes after trypsin digestion were carefully analyzed in order to detect differences. In silico estimation of the *m/z* ratio of the peptides after ZmC_4-NADP-ME trypsin digestion was considered in order to identify the peptides containing cysteine residues (**Supplementary Table S1**).

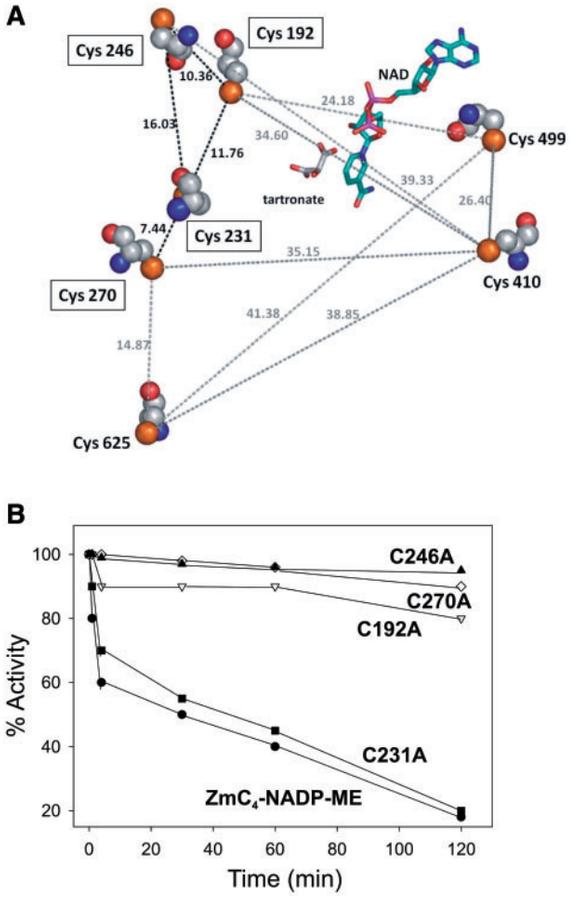

Fig. 3 (A) Three-dimensional model view of ZmC_4-NADP-ME. The predicted model was obtained using human mitochondrial NAD(P)-ME complexed with NAD, and tartronate used as a malate analog (1EFL from the Protein Data Bank; http://www.rcsb.org/pdb/). Relative distances among the seven cysteine residues are indicated in Ångstroms. Cys192, Cys231, Cys246 and Cys270 are highlighted as they display the lowest distances between each other and were further selected for mutagenesis analysis. (B) Redox modulation of ZmC_4-NADP-ME mutant activity. Purified recombinant ZmC_4-NADP-ME and C192A, C231A, C246A and C270A were incubated with 1 mM IBZ. At the indicated times, NADP-ME activity was measured and expressed as a percentage of the initial activity. For each time course incubation experiment, typical results are shown from at least three different incubation experiments using different purification batches, in which similar results were obtained. In each incubation experiment, the activity was measured once at the indicated time intervals. The initial activity of ZmC_4-NADP-ME was 200 ± 15 U mg^{-1}; 15 ± 0.6 U mg^{-1} for C231A; 4.0 ± 0.2 U mg^{-1} for C192A; and 1.0 ± 0.06 U mg^{-1} for C270A and C246A.

Signals for peptides containing Cys231 and Cys625 were clearly detected in both red- and oxZmC4-NADP-ME spectra (**Fig. 4**). Signals for the peptide containing Cys499 were also detected in both spectra, although that in the oxidized form was very small. In contrast, the signal for the peptide containing Cys410 was detected only in the case of redZmC4-NADP-ME (**Fig. 4**). In the case of the $oxZmC_4$-NADP-ME spectrum, no peak was detected with the *m/z* ratio corresponding to this peptide (**Fig. 4**). The identity of peptides containing Cys231, Cys410 (from $redZmC_4$-NADP-ME), Cys499 and Cys625 was corroborated by MS/MS analysis. Finally, no signals with the predicted *m/z* ratio could be detected for peptides containing Cys192, Cys246 or Cys270 either in the $redZmC_4$-NADP-ME or in the $oxZmC_4$-NADP-ME spectrum (not shown), which may be due, for example, to high *m/z* ratios, the presence of more than one peptide with similar *m/z* ratios, or improper trypsinization of the protein near these residues.

Discussion

The two maize plastidic NADP-MEs display distinct susceptibility to redox modulation

Redox regulatory mechanisms are essential in chloroplasts, where the activity of numerous enzymes is linked to the redox status of the photosynthetic electron transport chain (Buchanan and Balmer 2005). In the present work, the two maize plastidic NADP-MEs were analyzed regarding the redox modulation of their activities. The results obtained clearly show a distinct redox modulation of the two plastidic ZmNADP-MEs, the photosynthetic enzyme (ZmC_4-NADP-ME) being the only one modulated by the redox status (**Figs. 1A**, **5**). Loss of activity in ZmC_4-NADP-ME occurs concomitantly with the oxidation of thiol groups to disulfide bonds, as the oxidation is reversed by incubation with reductant agents (**Fig. 1B**). ZmC_4-NADP-ME oxidation produces a decrease in the maximum catalytic activity of the enzyme, which is associated with an increase in the affinity for both malate and NADP (**Table 1**, **Fig. 5**). Thus, enzyme oxidation produces a conformational change that limits the catalytic process although inducing a higher affinity binding of the substrate.

The results obtained suggest that, although the two ZmNADP-MEs share the same subcellular compartment, they display divergent properties that may be linked to a particular metabolic function in vivo. Thus, under oxidative conditions, $ZmnonC_4$-NADP-ME could be fully active, while ZmC_4-NADP-ME would be partially inactivated. It may be proposed that under conditions linked to oxidative processes, such as senescence or stress, $ZmnonC_4$-NADP-ME would be responsible for malate oxidative decarboxylation in plastids. Besides, an enzyme for malate oxidative decarboxylation not susceptible to oxidation may be required in non-photosynthetic plastids where $ZmnonC_4$-NADP-ME is the only ME expressed (Saigo et al. 2004; **Fig. 5**). Moreover, the reversible modulation of ZmC_4-NADP-ME may be important for fine-tuning of the C_4 metabolic pathway, as discussed below.

//Blrnas1/journals/application/oup/PCP/pcs059.3d [28.4.2012-4:21am] [1–10] Paper: pcs059
MANUSCRIPT CATEGORY: REGULAR PAPER

Identification of cysteine residues involved in the redox modulation of ZmC_4-NADP-ME

In the present work, two approaches were applied in order to identify the residues involved in the redox modulation of ZmC_4-NADP-ME activity: site-directed mutagenesis and MALDI-TOF-MS analysis of red- and oxZmC_4-NADP-ME (**Figs. 3**, **4**).

The predicted three-dimensional model of ZmC_4-NADP-ME indicated that only four cysteine residues (Cys192, Cys231, Cys246 and Cys270) out of the seven residues would be close enough to be involved in a disulfide bridge (**Fig. 3A**). Thus, these four cysteine residues were replaced by alanine and the corresponding mutated NADP-MEs were characterized. The four mutants display significantly lower catalytic efficiency than the wild type (**Table 2**), indicating the relevance of the cysteine residues for the maximum catalytic performance of the enzyme. When analyzing the redox modulation of activity of the four cysteine mutants, the results indicate that mutation of either Cys192, Cys246 or Cys270 to alanine prevents the loss of activity upon exposure to oxidative agents (**Fig. 3B**). However,

Table 2 Kinetic parameters of the recombinant wild-type NADP-ME and site-directed mutants

	k_{cat} (s^{-1})	K_m NADP (μM)	k_{cat}/K_m NADP	K_m malate (mM)	k_{cat}/K_m malate
redZmC_4-NADP-ME	269.0 ± 0.5	27.6 ± 1.2	9.7	0.39 ± 0.03	690
C192A	5.6 ± 0.3	15.4 ± 1.2	0.36	3.0 ± 0.12	1.9
C231A	23.2 ± 1.6	15 ± 0.9	1.5	1.70 ± 0.08	13.6
C246A	1.1 ± 0.06	5.3 ± 0.51	0.21	0.14 ± 0.01	7.8
C270A	1.6 ± 0.08	13.5 ± 0.8	0.12	4.30 ± 0.2	0.37

Purified recombinant ZmC_4-NADP-ME was treated with either 10 mM DTT (redZmC_4-NADP-ME) for 2 h or 2 mM diamide (oxZmC_4-NADP-ME) for 20 min. After the treatment, the enzyme was desalted and kinetic parameters were estimated at pH 8.0 or 7.0. Values are given as average ± SD. Each value is the average obtained using at least three different preparations of each enzyme.

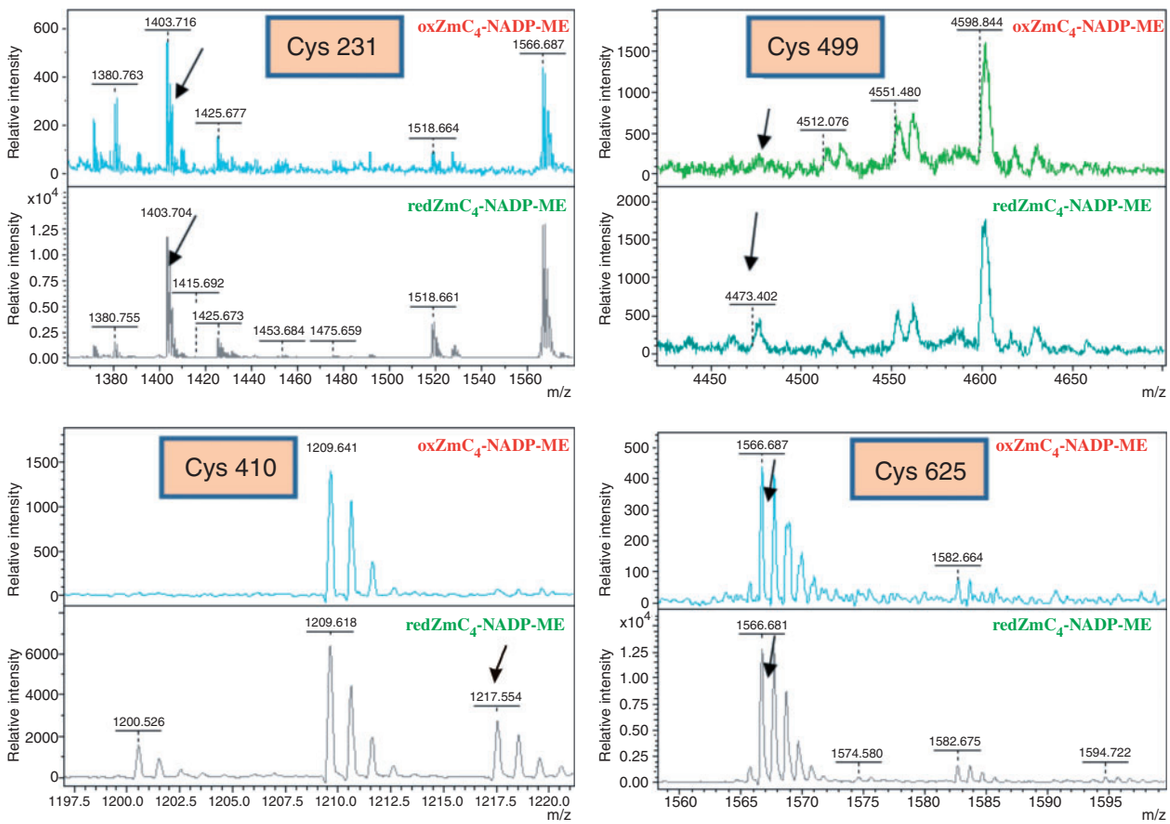

Fig. 4 Portions of MALDI mass spectra of the trypsinized redZmC_4-NADP-ME and oxZmC_4-NADP-ME. Each panel shows the portion of the spectrum with the signals for peptides containing cysteine residues for oxZmC_4-NADP-ME (treated with 2 mM diamide, top) and redZmC_4-NADP-ME (treated with 10 mM DTT, bottom). The arrow in each panel indicates signals for peptides containing Cys231, Cys410, Cys499 or Cys625.

//Blrnas1/journals/application/oup/PCP/pcs059.3d [28.4.2012–4:21am] [1–10] Paper: pcs059
MANUSCRIPT CATEGORY: REGULAR PAPER

mutation of Cys231 to alanine does not prevent oxidation at all (**Fig. 3B**). These results clearly indicate that Cys231 is not involved in ZmC_4-NADP-ME redox modulation, although it is implicated in the kinetic mechanism and/or binding of substrates (**Table 2**). Furthermore, these results indicate that Cys192, Cys246 and Cys270 contribute to the changes leading to ZmC_4-NADP-ME inactivation by oxidation, and may be directly involved in forming a disulfide bridge. Additionally, it may also be possible that mutation of one of these residues may induce a conformational change in the enzyme that prevents oxidation, for example increasing the distance between the cysteine residues involved in the disulfide bridge, and thus impeding bridge formation.

Regarding the MALDI-TOF-MS analysis of red- and $oxZmC_4$-NADP-ME, the results indicate that Cys231, Cys499 and Cys625 are not involved in the redox modulation of the enzyme, as the peptides containing these residues are found in both red- and $oxZmC_4$-NADP-ME spectra (**Fig. 4**). Moreover, the presence of the peak corresponding to the peptide containing Cys410 only in $redZmC_4$-NADP-ME, and not in $oxZmC_4$-NADP-ME, indicates the participation of this residue in the formation of a disulfide bridge (**Fig. 4**). Unfortunately, the peaks for peptides containing Cys192, Cys246 and Cy270 could not be detected under any condition, which could be due, for example, to the high *m*/*z* ratio of the peptide containing Cys270, the presence of a lysine at the end of the peptide containing Cys192 or the presence of more than one peptide with similar *m*/*z* ratios (this was the case for the peptide containing Cys246).

Overall, considering the two approaches used, it can be postulated that Cys192, Cys246, Cys270 and Cys410 are directly or indirectly involved in the redox modulation of ZmC_4-NADP-ME. Several hypotheses agree with the results obtained. First, a disulfide bridge between Cys410 and one of the other three cysteine residues partially inactivates the enzyme, and the mutation of the two remaining cysteine residues induces a conformational change that avoids the oxidation of the enzyme to form the bridge. Secondly, the four cysteine residues contribute to the formation of disulfide bridge(s), maybe by producing alternative disulfide bonds or by additive effects. In this regard, it is also worth mentioning that the replacement of Cys246 with serine in $ZmnonC_4$-NADP-ME (**Fig. 2**) may be responsible for the absence of redox modulation (**Fig. 1A**). In this sense, when analyzing the two putative plastidic NADP-MEs (SbME1 and -2) from *Sorghum bicolor*, another C_4 species that uses NADP-ME as the main decarboxylase in BSCs, it is also notable that the residue homologous to Cys246 is found in only one of the two isoforms (**Supplementary Fig. S3**). Notably, the isoform with a cysteine at position 246 is the one exhibiting the highest degree of identity with the maize photosynthetic enzyme (**Supplementary Fig. S3**). In this way, it is possible that the redox modulation of NADP-MEs is a feature needed for the fine-tuning of the C_4 flux in the photosynthetic process.

Finally, the participation of Cys410 in the disulfide bond of ZmC_4-NADP-ME (**Fig. 4**) was rather surprising when considering the three-dimensional model of this enzyme (**Fig. 3A**). However, it is worth noting that this model was constructed using non-plant NADP-MEs, which show several and relevant sequence differences with plant NADP-MEs (Detarsio et al. 2004, Detarsio et al. 2007). Moreover, from the seven cysteine residues of ZmC_4-NADP-ME, only three (Cys192, Cys270 and Cys499) are conserved in human mitochondrial NAD(P)-ME (not shown). Therefore, the three-dimensional model of ZmC_4-NADP-ME used in the present work may not precisely reflect the real tertiary structure of the enzyme, making it necessary to collect crystallographic data for plant NADP-MEs and refine the modelling analysis.

Redox modulation in BSC chloroplasts for C_4-NADP-malic enzymes?

In the present work, the redox modulation for an enzyme exclusively localized in maize BSC chloroplasts and involved in C_4 photosynthesis is presented. Previous work described an increase in NADP-ME activity due to illumination of leaves with the participation of redox processes (Drincovich and Andreo 1994, Murmu et al. 2003). When using maize leaf discs, the increase in NADP-ME activity after illumination was due, at least in part, to the reduction of dithiols, indicating a change in the activation state of the enzyme (Murmu et al. 2003; **Fig. 5**). However, when considering the relevance of such regulation in vivo, it must be taken into account that maize BSC chloroplasts show low levels of active PSII complexes and only limited amounts of NADPH production from linear photosynthetic electron transport, NADP-ME being the main source of reducing power for BSC chloroplasts (Majeran and van Wijk 2009). It is interesting to note that recent proteomic studies comparing maize mesophyll and BSC chloroplasts have indicated the compartmentalization of several redox regulators and antioxidative defense systems, quantifying higher expression levels of several redox regulators in the mesophyll, with the exception of some BSC-specific components (Majeran et al. 2005, Majeran and van Wijk 2009). These results raise the question of whether the bundle sheath and mesophyll redox activation systems are specific for some particular enzymes, and also if some of the BSC-specific components are involved in maintaining ZmC_4-NADP-ME in its reduced state.

The operation of the C_4 photosynthetic pathway requires a deep synchronization between mesophyll and BSCs (Bailey et al. 2007). For C_4 photosynthesis to concentrate CO_2 around RubisCO in BSC chloroplasts, the NADP-ME decarboxylation and RubisCO carboxylation rates must be coordinated to avoid leakage of the CO_2 produced by NADP-ME. Moreover, the carboxylation (in mesophyll cells) and decarboxylation (in BSCs) reactions must be also regulated to accommodate the large and rapid flux changes that occur during photosynthesis. In this regard, the relevance of the light activation of NADP-malate dehydrogenase from *S. bicolor*, mediated by thioredoxin, which occurs in mesophyll cells of this C_4 species is well known (Goyer et al. 2001). Another example

//Blrnas1/journals/application/oup/PCP/pcs059.3d [28.4.2012–4:21am] [1–10] Paper: pcs059
MANUSCRIPT CATEGORY: REGULAR PAPER

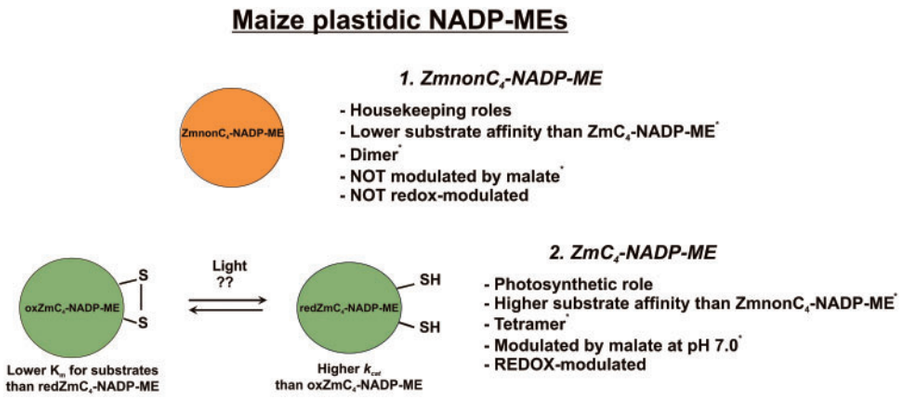

Fig. 5 Scheme showing the most relevant differences between the plastidic isoforms ZmnonC$_4$-NADP-ME and ZmC$_4$-NADP-ME. Properties indicated with an asterisk (*) were previously described in Detarsio et al. (2007). As presented in this work, ZmC$_4$-NADP-ME is the only isoform that can be reversibly reduced with changes in its catalytic properties (**Table 1**). As indicated in Murmu et al (2003), one of the signals that is able to mediate the reduction of NADP-ME in vivo is light, which is indicated in the figure.

is the redox regulation by thioredoxin of glycerate 3-kinase in maize mesophyll cells, an enzyme participating in photorespiration (Bartsch et al. 2010). Thus, modulation of ZmC$_4$-NADP-ME activity by the redox state appears to be a suggestive regulatory mechanism for enzyme adaptation to the changing functional status of the BSC chloroplasts. It may be possible that activation of ZmC$_4$-NADP-ME by reduction of thiol groups occurs under light or reductive conditions in BSC chloroplasts to allow a fine-tuning of the flux through the C$_4$ pathway (**Fig. 5**). In this way, when photosynthesis is operating, ZmC$_4$-NADP-ME displays its maximum catalytic activity. Although more C$_4$ -NADP-ME family members should be analyzed, it is probable that the redox modulation of this enzyme was a critical step towards the evolution to C$_4$ NADP-MEs. Therefore, the present work provides new insights towards the understanding of the regulation of C$_4$ enzymes, which is crucial for fully exploiting the potential of this type of metabolism (Hibberd et al. 2008, Hibberd and Covshoff 2010).

Materials and Methods

Site-directed mutagenesis of ZmC$_4$-NADP-ME

Site-directed mutagenesis of maize mature NADP-ME was carried out according to the procedure of Mikaelian and Seargeant (1992). The primers that introduced mutations in the wild-type protein were as follows: C192A, 5′-AGGTGAGGC**CGC**CCAGAA GTAT-3′; C232A, 5′-TCAAGTTAT**CGC**TGTTACTGATGGTGA G-3′; C246A, 5′-GGAGATTTGGG**TGC**TCAGGGAATG-3′; and C290A, 5′-GACCCATCAGT**TGC**CTTGCCTATC-3′. The mutated positions are in bold in the oligonucleotide sequence. These mutagenic primers were used in combination with the following primers in order to obtain the complete sequence of NADP-ME: 5EMMut, 5′-TAGCATGCCATGGCGATG-3′; and 3EMMut, 5′-CAACGCTCGAGGCACTACC-3′. PCR was carried out using a mixture of *Taq* and *Pfu* polymerases (10 : 1) in order to minimize possible errors introduced by *Taq* polymerase. The resulting sequences obtained by PCR were purified from agarose gels. These fragments were used as megaprimers, in combination with the 5EMMut and 3EMMut primers, to amplify the complete sequences. The resulting fragments were separated on agarose gels, purified by QIAprep columns (Qiagen) and ligated into pGEMT-Easy vectors (Promega). The introduced sequences were checked to verify the presence of the desired mutations and that no errors were added due to PCR and subcloning procedures. The different sequences obtained were cloned into pET32a vectors (Novagen).

Expression and purification of recombinant NADP-MEs

Escherichia coli BL21(DE3) cells were transformed with the pET32 plasmids containing the mutated NADP-MEs. The resulting fusion proteins were purified using a His-Bind column (Novagen). Induction and purification of the mutated proteins were performed as previously described for the photosynthetic NADP-ME (Detarsio et al. 2003). Fusion enzymes were then concentrated on Millipore MW-30 (Amicon) and desalted using a buffer containing 100 mM Tris pH 8.0 and 10 mM $MgCl_2$. Purified enzymes were stored at −80°C with the addition of 50% glycerol. ZmC$_4$-NADP-ME and ZmnonC$_4$-NADP-ME were purified as previously described (Detarsio et al. 2003, Saigo et al. 2004, Detarsio et al. 2007).

Redox modulation of the activity of recombinant NADP-MEs

The different purified recombinant NADP-MEs (approximately 50 μg) were incubated at 0°C in buffer containing 100 mM Tris–HCl (pH 8.0) and 10 mM $MgCl_2$ with different redox compounds (1 mM IBZ, 25 μM $CuCl_2$, 2 mM diamide or 10 mM DTT). At different incubation times, aliquots were withdrawn and assayed for NADP-ME activity. Modification of the

recombinant enzymes was stopped by dilution (at least 100-fold) of redox compounds in the assay media. No significant decrease in activity was found when the recombinant NADP-MEs were incubated in the absence of redox compounds. Addition of these compounds (100-fold diluted) to the NADP-ME assay medium had no significant effect on the enzyme activity assay.

NADP-ME activity assay and estimation of kinetic parameters

NADP-ME activity was measured spectrophotometrically at 30°C by monitoring NADPH production at 340 nm. The standard reaction mixture contained 100 mM Tris–HCl pH 8.0 (or 7.0 when stated), 10 mM $MgCl_2$, 0.5 mM NADP and 4 mM L-malate. The reaction was started by the addition of L-malate. One unit is defined as the amount of enzyme that catalyzes the formation of 1 μmol of NADPH min^{-1} under the specified conditions. Initial velocity studies were performed by varying the concentration of one of the substrates around its K_m while keeping the remaining substrate concentrations at saturating levels. All kinetic parameters were calculated at least in triplicate and subjected to non-linear regression, using free concentrations of all substrates (Detarsio et al. 2003). Kinetic parameters of NADP-ME were also obtained after treatment with either 10 mM DTT (redZmC_4-NADP-ME) for 2 h or 2 mM diamide (oxZmC_4-NADP-ME) for 20 min at 0°C. After both treatments, the enzyme was desalted using Microcon MW-30 (Amicon) with 100 mM Tris–HCl pH 8.0 and 10 mM $MgCl_2$.

Gel electrophoresis

SDS–PAGE was performed in 8% or 10% (w/v) polyacrylamide gels according to Laemmli (1970). Proteins were visualized by Coomassie Blue staining. Native PAGE was performed employing a 6% (w/v) polyacrylamide separating gel (Detarsio et al. 2007).

Mass spectrometry of red- and oxZmC_4-NADP-ME

Approximately 20 μg of redZmC_4-NADP-ME or oxZmC_4-NADP-ME was run on a 10% (w/v) polyacrylamide SDS–PAGE in the absence of any reductant. Coomassie-stained bands were excised from the gel and treated with 10 mM iodoacetamide to block thiol groups by carbamidomethylation. MS data from tryptic digestion of SDS–polyacrylamide gel bands were obtained by using a MALDI-TOF spectrometer, Ultraflex II (Bruker), in the MS facility CEQUIBIEM (Centro de Estudios Químicos y Biológicos por Espectrometría de Masa; Facultad de Ciencias Exactas y Naturales, Universidad de Buenos Aires, Argentina). Spectra obtained from redZmC_4-NADP-ME or oxZmC_4-NADP-ME were manually evaluated and compared with the in silico digestion predicted peptides of redZmC_4-NADP-ME (**Supplementary Table S1**). Peaks of putative peptides containing cysteine residues were sequenced for verification. At least two different preparations of redZmC_4-NADP-ME or oxZmC_4-NADP-ME were used for MS analysis.

Supplementary data

Supplementary data are available at PCP online.

Funding

This work was supported by Agencia Nacional de Promoción Científica y Tecnológica [PICT 2164, Argentina]; Consejo Nacional de Investigaciones Científicas y Técnicas (CONICET, Argentina).

Acknowledgments

The authors want to thank Dr. A. Vila (IBR, Rosario, Argentina) for kindly facilitating the CD apparatus. C.S.A., M.F.D. and S.M. are members of the Researcher Career of CONICET and C.E.A. is a fellow of the same institution.

References

Bailey, K.J., Gray, J.E., Walker, R.P. and Leegood, R.C. (2007) Coordinate regulation of phosphoenolpyruvate carboxylase and phosphoenolpyruvate carboxykinase by light and CO_2 during C4 photosynthesis. *Plant Physiol.* 144: 479–486.

Bartsch, O., Mikkat, S., Hagemann, M. and Bauwe, H. (2010) An autoinhibitory domain confers redox regulation to maize glycerate kinase. *Plant Physiol.* 153: 832–840.

Buchanan, B.B. and Balmer, Y. (2005) Redox regulation: a broadening horizon. *Annu. Rev. Plant Biol.* 56: 187–220.

Detarsio, E., Andreo, C.S. and Drincovich, M.F. (2004) Basic residues play key roles in catalysis and $NADP^+$-specificity in maize (*Zea mays* L.) photosynthetic $NADP^+$-dependent malic enzyme. *Biochem. J.* 382: 1025–1030.

Detarsio, E., Alvarez, C., Saigo, M., Andreo, C.S. and Drincovich, M.F. (2007) Identification of domains involved in tetramerization and malate inhibition of maize C4-NADP-malic enzyme. *J. Biol. Chem.* 282: 6053–6060.

Detarsio, E., Gerrard Wheeler, M., Campos Bermúdez, M.V., Andreo, C.S. and Drincovich, M.F. (2003) Maize C4 NADP-malic enzyme. Expression in *Escherichia coli* and characterization of site-directed mutants at the putative nucleoside-binding sites. *J. Biol. Chem.* 278: 13757–13764.

Detarsio, E., Maurino, V.G., Alvarez, C., Muller, G., Andreo, C.S. and Drincovich, M.F. (2008) Maize cytosolic NADP-malic enzyme (ZmCytNADP-ME): a phylogenetically distant isoform specifically expressed in embryo and emerging root. *Plant Mol. Biol.* 68: 355–367.

Drincovich, M.F. and Andreo, C.S. (1992) A study on the inactivation of maize leaves NADP-malic enzyme by 3-bromopyruvate. *Phytochemistry* 31: 1883–1888.

Drincovich, M.F. and Andreo, C.S. (1994) Redox regulation of maize NADP-malic enzyme by thiol–disulfide interchange: effect of reduced thioredoxin on activity. *Biochem. Biopys. Acta* 1206: 10–16.

Drincovich, M.F., Casati, P. and Andreo, C.S. (2001) NADP-malic enzyme from plants: a ubiquitous enzyme involved in different metabolic pathways. *FEBS Lett.* 490: 1–6.

Drincovich, M.F., Lara, M.V., Andreo, C.S. and Maurino, V.G. (2011) C_4 decarboxylases: different solutions for the same biochemical problem, the provision of CO_2 to RubisCO in the bundle sheath cells. *In* C_4 Photosynthesis and Related CO_2 Concentrating Mechanism. Edited by Raghavendra, A.S. and Sage, R.F. pp. 277–300. Springer Science, Dordrecht, The Netherlands.

Drincovich, M.F., Spampinato, C.P. and Andreo, C.S. (1992) Evidence for the existence of two essential and proximal cysteinyl residues in NADP-malic enzyme from maize leaves. *Plant Physiol.* 100: 2035–2040.

Edwards, G.E. and Andreo, C.S. (1992) NADP malic enzyme from plants. *Phytochemistry* 31: 1845–1857.

Goyer, A., Decottignies, P., Issakidis-Bourguet, E. and Miginiac-Maslow, M. (2001) Sites of interaction of thioredoxin with sorghum NADP-malate dehydrogenase. *FEBS Lett.* 505: 405–408.

Hibberd, J.M., Sheehy, J.E. and Langdale, J.A. (2008) Using C_4 photosynthesis to increase the yield of rice—rationale and feasibility. *Curr. Opin. Plant Biol.* 11: 228–231.

Hibberd, J.M. and Covshoff, S. (2010) The regulation of gene expression required for C_4 photosynthesis. *Annu. Rev. Plant Biol.* 61: 181–207.

Kanai, R. and Edwards, G. (1999) The biochemistry of C4 photosynthesis. *In* C4 Plant Biology. Edited by Sage, R.F. and Monson, R.K. pp. 411–444. Academic Press, San Diego.

Kosower, N.S. and Kosower, E.M. (1987) Formation of disulfides with diamide. *Methods Enzymol.* 143: 264–270.

Ku, M.S.B., Kano-Murakami, Y. and Matsuoka, M. (1996) Evolution and expression of C4 photosynthesis genes. *Plant Physiol.* 111: 1251–1261.

Laemmli, U.K. (1970) Cleavage of structural proteins during the assembly of the head of bacteriophage T4. *Nature* 227: 680–685.

Majeran, W., Cai, Y., Sun, Q. and van Wijk, K.J. (2005) Functional differentiation of bundle sheath and mesophyll maize chloroplast determined by comparative proteomics. *Plant Cell* 17: 3111–3140.

Majeran, W. and van Wijk, K.J. (2009) Cell-type-specific differentiation of chloroplast in C4 plants. *Trends Plant Sci.* 14: 100–109.

Maurino, V.G., Drincovich, M.F., Casati, P., Andreo, C.S., Edwards, G.E., Ku, M.S.B. et al. (1997) NADP-malic enzyme: immunolocalization in different tissues of the C4 plant maize and the C3 plant wheat. *J. Exp. Bot.* 48: 799–811.

Maurino, V.G., Saigo, M., Andreo, C.S. and Drincovich, M.F. (2001) Non-photosynthetic malic enzyme from maize: a constitutively expressed enzyme that responds to plant defense inducers. *Plant Mol. Biol.* 45: 409–420.

Mikaelian, I. and Sergeant, A. (1992) A general and fast method to generate multiple site directed mutagenesis. *Nucleic Acids Res.* 20: 376.

Murmu, J., Chinthapalli, B. and Raghavendra, A.S. (2003) Light activation of NADP malic enzyme in leaves of maize: marginal increase in activity, but marked change in regulatory properties of enzyme. *J. Plant Physiol.* 160: 51–56.

Rothermel, B.A. and Nelson, T. (1989) Primary structure of the maize NADP dependent malic enzyme. *J. Biol. Chem.* 264: 19587–19592.

Saigo, M., Bologna, F., Maurino, V.G., Detarsio, E., Andreo, C.S. and Drincovich, M.F. (2004) Maize recombinant non-C4 NADP-malic enzyme: a novel dimeric enzyme with high specific activity. *Plant Mol. Biol.* 55: 97–107.

Tausta, S.L., Coyle, H.M., Rothermel, B., Stiefel, V. and Nelson, T. (2002) Maize C4 and non-C4-dependent malic enzymes are encoded by distinct genes derived from a plastid-localized ancestor. *Plant Mol. Biol.* 50: 635–652.